Morphology, composition, and structure of carbon deposits from diesel and biomass oil/diesel blends on a pintle-type fuel injector nozzle

Wo, Hengzhou; Dearn, Karl D.; Song, Ruhong; Hu, Enzhu; Xu, Yufu; Hu, Xianguo

DOI:
10.1016/j.triboint.2015.07.003

Document Version
Peer reviewed version

Citation for published version (Harvard):
Wo, H, Dearn, KD, Song, R, Hu, E, Xu, Y & Hu, X 2015, 'Morphology, composition, and structure of carbon deposits from diesel and biomass oil/diesel blends on a pintle-type fuel injector nozzle', *Tribology International*, vol. 91, pp. 189-196. https://doi.org/10.1016/j.triboint.2015.07.003

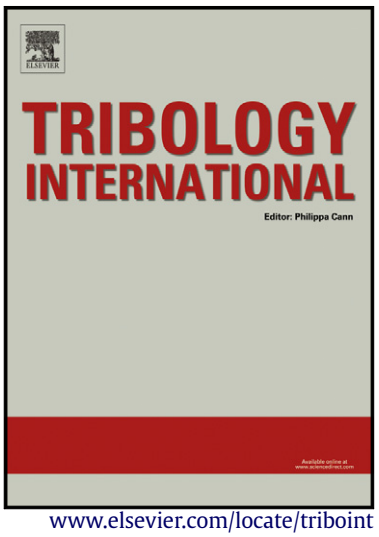

www.elsevier.com/locate/triboint

Morphology, composition, and structure of carbon deposits from diesel and biomass oil/diesel blends on a pintle-type fuel injector nozzle

Hengzhou Wo, Karl D. Dearn, Ruhong Song, Enzhu Hu, Yufu Xu, Xianguo Hu

PII: S0301-679X(15)00288-1
DOI: http://dx.doi.org/10.1016/j.triboint.2015.07.003
Reference: JTRI3738

To appear in: *Tribology International*

Received date: 22 December 2014
Revised date: 10 June 2015
Accepted date: 3 July 2015

Cite this article as: Hengzhou Wo, Karl D. Dearn, Ruhong Song, Enzhu Hu, Yufu Xu, Xianguo Hu, Morphology, composition, and structure of carbon deposits from diesel and biomass oil/diesel blends on a pintle-type fuel injector nozzle, *Tribology International,* http://dx.doi.org/10.1016/j.triboint.2015.07.003

Morphology, composition, and structure of carbon deposits from diesel and biomass oil/diesel blends on a pintle-type fuel injector nozzle

Hengzhou Wo[1], Karl D. Dearn[2], Ruhong Song[1], Enzhu Hu[1], Yufu Xu[1], Xianguo Hu[1,*]

[1] *School of Mechanical and Automotive Engineering, Hefei University of Technology, Hefei 230009, P. R. China*

[2] *School of Mechanical Engineering, University of Birmingham, B15 2TT, United Kingdom*

Abstract

A biomass oil/diesel blend was prepared using an emulsion method and combusted in a diesel engine. An injector was then removed and the morphology, composition, and structure of the carbonaceous deposits on the pintle-type nozzle were characterized using a combination of HRTEM, SEM/EDAX, Raman and XRD. Results showed that the carbon deposition of the emulsified fuel with high crystallinity was greater than that of diesel. The agglomerated particulate diameters of the deposited carbon from diesel and emulsified fuel were approximately 10-30 μm and 50 μm, respectively. The carbon deposition mechanism from the emulsified fuel was attributed to the high oxygen content of the groups leading to increased polymerization and subsequent condensation on the nozzle surfaces that was then carbonised.

Keywords: biomass-oil, diesel, carbon deposit, nozzle

* Corresponding author: Tel/Fax: +86 551 62901359; e-mail: xghu@hfut.edu.cn (X. Hu)

1. Introduction

There are two potential energy sources that are needed to sustain life and human development: renewable energy, such as that derived from solar, biomass, and wind energy, and non-renewable energy, such as coal, petroleum, and natural gas [1–3]. The rapid development of society and gradual reduction of non-renewable energy sources have negatively affected the energy supply of the world. Biomass, which is a renewable energy source, has received considerable research attention because of its wide distribution, large reserves, low cost, and ease of use. The exploitation and application of biomass energy has important economic and environmental benefits to society [4].

The liquefaction or gasification processes of biomass can be used to produce biomass oil or gas. Biomass oils are directly combusted to produce electricity and heat. The resulting substance can be used as an alternative fuel for diesel or gasoline engines and the use of biomass oil as an engine fuel has been gradually gaining acceptance [5–7]. Fast liquefaction biomass fuel has become one of the most important alternative fuels. Zhu et al. [8] utilized the fast liquefaction method to convert straw and rice husks into biomass crude oils, which are eco-friendly, renewable, and can be used as alternative fuels. However, the use of biomass crude oil produces soot, which can affect engine performance and emissions. Thus, biomass crude oil must be upgraded for modern engines. Emulsion is one of the most effective upgrading methods for obtaining an acceptable performance from alternative fuels [9, 10]. Biomass crude oil also plays an important role in the wear and friction of engine parts through polymerization, oxidization, condensation, and corrosion reactions [11, 12]. Hu et al. [13] investigated the wear and friction characteristics of biomass crude oil. Their results show that biomass derived fuels have a better lubrication performance compared with diesel. The lubrication performance of biomass crude oil was ascribed to the reaction of active functional groups with metals in forming boundary lubrication films.

One by-product of fuel combustion is carbon, the black soot that can collect and harden on critical engine components such as the cylinder head, cylinder wall, piston and valves. Carbon deposits in the combustion chamber can affect engine performance, including tribological properties, which results in higher oil consumption, engine knock and overheating. The morphology, composition, and structure of carbonaceous deposits should be considered for the wear and heat transfer of engine parts when biomass oils are used in engines [14]. Numerous studies have focused more on carbon deposits generated from a range of conventional and alternative engine fuels but less so with biodiesel derived deposits. Uy *et. al.* [15] characterized the nanostructure of gasoline soot. They determined and

compared the degree of order of the graphitic planes of soot's primary particles extracted from the exhaust gas and from engine oil. Further, a recent study on soot agglomerates showed that centrifugation altered the distribution of size and shape of these particles [16]. Fuel additives can also effect the composition and formation of carbonaceous deposits. For example, Baker et al. in a series of papers performed engine tests using commercial and non-commercial low molecular weight polyisobutylenesuccinimide (PIBSI) as an engine fuel additive. They observed 'sticking' of needle valves within some injectors [17] and following spectroscopic analysis, postulate that formation is complex and multifaceted. Further tests using a commercial grade PIBSI detergent showed that sticking was eliminated. They describe the aromatic structure of internal diesel injector deposits (IDID) [18] and reviewed the development of diesel injector deposit theory as it has evolved with the engine technology in the light of their findings [19]. Mendiratta et al. [20] indicated that engine oils contribute significantly to the formation of carbon deposits. The basic parameters involved in deposit formation are surface temperature, engine operating conditions, and condensation and polymerization of engine oil components. Parsinejad et al. [21] investigated the characteristics of carbon deposits on different types of injector nozzle by using elemental and thermal analytical techniques; both fuel and engine lubricants contributed to the composition of deposits. The deposit composition on a direct-injection spark-ignition (DISI) intake valve consisted of 10 wt% or higher non-C (inorganic) elements wherein Ca, Mo, Zn, P, and S were dominant. The number of inorganic elements in the DISI intake valve deposit was at least one order of magnitude higher than that in the port fuel injection intake valve deposit. Analysis data showed that significant differences existed in the deposit volatility and inorganic component quantity between the combustion chamber deposits produced from Group III base oil (lower) and poly-alpha-olefin (PAO) base oil (higher). No correlation was observed between the sulfated ash value of the lubricating oil and elemental composition of the deposits.

Several studies have also been conducted to classify deposit structures [22-24]. Researchers found that generally carbon material was amorphous, porous, and characterized by a heterogeneous granular structure. Studies have been conducted by using transmission electron microscopy [13], C solid-state nuclear magnetic resonance, Fourier transform infrared spectroscopy, gas chromatography–mass spectrometry , and other techniques. The heterogeneity of the deposit structures, which were composed of unburned hydrocarbon chains and varying amounts of O, C, K, and Ca, made the analysis complex. Substantial variations existed in the composition of deposits from different parts of the combustion chamber.

No reports have been made on C deposits in engine nozzles when emulsified biomass oil is used with diesel, blended as alternative fuel. The present paper studied the morphology, composition, and structure of C deposits formed as a result of the combustion of an emulsified biomass oil /diesel blend, on a pintle-type nozzle. This study aimed to understand the performance of C deposition and the formation mechanism of emulsified biomass oil derived deposits.

2. Materials and methods

2.1. Materials

The Key Laboratory for Biomass Clean Energy of Anhui Province in China produced liquid biomass oil using the fast pyrolysis of rice husks. A commercial diesel fuel (0#) was purchased from China Sinopec Corporation for reference. Distilled–refined biomass oils were obtained by the reduced-pressure method with a vacuum value of −0.1 MPa at 78 °C. All other chemical reagents were of analytical grade.

The biomass oil/diesel blend was prepared by mixing the diesel with distilled–refined biomass oils, using a high shear emulsion machine (model SG×400). The detailed preparation procedure for the blend was as follows: 1.02 g emulsifier (Span-80) was added into 1.0 g biomass oil. Thereafter, a 0.98 g emulsifier (OP-10) was added into 97 g of $0^{\#}$ diesel fuel. The mixture was stirred until the liquid was uniform. The former mixture was slowly added into the latter mixture with a shear speed of 1500 rpm at 30 °C for 20 min. The physical and chemical properties of diesel and emulsified fuel are listed in **Table 1**.

Table 1

2.2 Engine tests

Engine tests were conducted using a mode S195 diesel engine test bench (Anhui Quanjiao Diesel Engine Co.), running with an emulsified biomass oil/diesel blend and $0^{\#}$ diesel under idle load condition for 10 hours respectively. The specification of the engine is given in **Table 2**. After running for 10 hours, the

injector nozzle was removed and the deposit analyzed. In addition to this, at the end of each test, a new injector nozzle was selected and installed. The engine was then flushed and a new lubricant was added for each test.

Table 2

Soot particles extracted from the engine oil were prepared using a solvent extraction process as outlined in [25] for each fuel combination. This entailed diluting the oil at a ratio of 1:60 in heptane, producing a solution containing much lower oil content, and also at a suitable low viscosity to allow deposition onto a carbon coated transmission electron microscope grid. During the sample preparation and following deposition, the solvent evaporates rapidly to leave soot particles of varying sizes and aggregations.

2.3. Characterization

Morphology, composition, and structural analyses were performed on the removed pintle nozzles by scanning electron microscopy/energy dispersion spectroscopy (SEM/EDS; JEOL Model JSM-6490), optical microscopy (OM; LY-WN-HPCCD), high resolution transmission electron microscope (HRTEM, JEOL JEM-2010 at an acceleration voltage of 200 kV), X-ray diffraction (XRD, Rigaku D/max-γB X-ray diffractometer with Cu-Kα radiation). Finally a Raman spectrometer (Raman, LabRAM-HR; resolution = 0.6 cm^{-1}, scanning repeatability = ±0.2 cm^{-1}) which consisted of a light microscope (Leica DL-LM; Olympus BX) with three different excitation lasers. Finally, the thickness of the deposited carbon layer was measured using a VK-X100/X200 Series 3D Laser Scanning Microscope, KEYENCE Corporation.

3. Results and discussion

3.1. Optical image analysis

Figure 1 shows the optical images of the injector nozzles and needle valves after the engine tests. Relating to the deposition on the nozzle, the use of 0# diesel resulted in less carbon than that from the emulsified biomass oil/diesel blend, this is confirmed by the XRD analysis show below.

The thicknesses of the deposited carbon from the diesel and emulsified biomass fuels were measured as 6.931 μm and 25.940μm respectively and are shown in figure 1.

Figure 1

For the needle valve, no ablation was observed on the sealing surface or the area near the needle valve regions, due to the high combustion temperatures when fuelled with diesel. The sealing surface of the needle valve was covered by a layer of carbon for the emulsified fuel, suggesting that the surface of the needle valve easily formed C deposits when emulsified fuel was used as the engine fuel. There is also evidence of the incomplete combustion of the emulsified fuel on the surface in the images. At these points, small molecules of the biomass oil formed high viscosity liquid molecules that adhered to the surface of the nozzle under high temperatures.

Figure 2

Figure 2 shows the OM images of the end face of the nozzles after the tests with the two fuels. The carbon deposition of emulsified fuel had a deep color and nest-like structure, which is consistent with the results mentioned above. The biomass oil in the blend is likely to have been absorbed on the nozzle surface and then combusted to form carbonaceous matter, which were mixed with the unburned biomass to form an adhesive body. The carbonaceous layer was uniform for the diesel fuel.

3.2. XRD analysis

The deposited C was underwent XRD analysis to investigate the formation mechanism of the carbon deposits. **Figure 3** shows the XRD analysis results of the two kinds of deposit. The diffraction pattern of the graphite-2H exhibits four distinct values in the 2θ from 10° to 60°, which can be indicated as 26.8°

(002), 44.5° (101), and 54.9° (102) according to the standard card PDF41-1487 database [26]. The diffraction pattern of the two samples exhibited only one broad reflection with intensity maxima at 19.9° and 21.5°. These findings suggest that the two carbonaceous materials did not have clear graphite-like structures [27], rather they were amorphous carbon; these findings are consistent with the results given in [28-30]. The carbon material of emulsified fuel showed higher crystallinity than that of diesel; this result was further evidenced by the peaks at 19.9° (002), and 43.5 (101) in the carbonaceous material of the emulsified fuel, as shown in **Figure 3.** Compared to the standard card PDF41-1487 database, the spectral peaks were lower and this is likely to be a result of a finer microcrystalline structure of the graphite. Based on the XRD analysis, the results showed that emulsified fuel resulted in a higher graphitic degree of carbon deposition than that of the diesel.

Figure 3
Table 3

Element analysis was conducted for the two C materials by atomic absorption spectrometry (Perkin Elmer Model AA800) to understand the mechanism of carbon deposition [31]. Detailed results are given in **Table 3.** The C and H contents in the carbonaceous deposit for the emulsified fuel were higher than that for diesel; as a result of the higher H_2O content and lower heat value. However, the higher heat value and lower H_2O content of diesel promoted complete combustion and minimal carbon deposition. The N content in the carbon deposit of the emulsified fuel was also higher because of the partial combustion of lubricating oil additives. The O content in the emulsified fuel deposits was less than that of diesel because diesel requires a higher oxygen content for combustion. The high O and H_2O content in the emulsified fuel caused incomplete combustion and was subsequently absorbed onto the nozzle surface.

3.3. SEM/EDS analysis

SEM (scanning electron microscopy) was used to observe the microstructures, and zones were selected to analyze the elemental contents. **Figure 4** shows the micro images of the end face of the needle valve seat after the two fuels were used. The carbon particulates from diesel were randomly dispersed. The average agglomerated particulate diameter was approximately 10 µm to 30 µm. No carbon particulates

were observed from emulsified fuel; however, large agglomerated matter was found on the surface of the needle valve seat. The agglomerated particulate matter diameter was approximately 50 μm. This significant agglomeration phenomenon was caused by the combination of carbon particulates and unburned fuel, thus forming a high viscosity mixture. The carbon deposit layer from the emulsified fuel appeared to be denser and thicker than that from diesel.

Figure 4
Figure 5

Figure 5 shows the micro images of the needle valve sealing surface after tests with the two fuels. No carbonaceous deposits were observed on the needle valve sealing surface for diesel. By contrast, numerous black oil-like impurities were observed on the surfaces for the emulsified fuel. These results indicate that the carbonaceous deposit was caused by the interaction between the unburned fuel and carbon particulates; this result was consistent with the abovementioned results.

EDS was used to obtain the element contents in the carbonaceous deposit to understand the deposition mechanism further. **Figure 6** shows the SEM images and EDS analysis region of the end face of the needle valve seat. The EDS analysis results are shown in **Table 4**.

Figure 6
Table 4

The results showed that the carbon deposits from the different fuels had similar elemental compositions, wherein the C content was 23.93 wt% for diesel and 25.87 wt% for the emulsified fuel. However, the O and P content varied. The occurrences of S, Zn, and K were attributed to the combustion of additives derived from the lubricating oil, which could have entered the combustion chamber via blow by or by bypassing the piston rings. Furthermore, while in the sump the diesel fuel can react with

the base oil, additive package or both, leading to the formation of oil sludge. It can also lead to a change in viscosity such that the lubricating oil can enter the chamber through the piston ring pack. Therefore, Zn was higher by up to 10.51 wt% in the C deposit from emulsified fuel. This result was possibly caused by the additives containing Zn in the lubricating oil, being catalyzed causing a weak lubrication condition and effecting engine operation. The actual reason for higher Zn concentration is not well understood due to the complex nature of biomass fuel. **Figure 7** and **Table 5** show the EDS analysis results of the C deposits on the needle valve with the two selected points (depicted by the crosses) from the emulsified fuel. Point cross-shaped in Figure 7 (a) was not covered with C deposits, whereas the point cross-shaped in Figure 7 (b) was covered with C deposits. The EDS spectra from the region not affected by C deposition showed that the main elements included C, Cr, Fe, and Co, which were consistent with the compositions of high-strength steel. The main elements from region covered with C deposits were C, Fe, O, S, Cl, K, Ca, and Zn. On the other hand, S, Cl, Ca, and Zn originated from the combustion of lubricating oil, and K was derived from the composition of biomass oil in the emulsified fuel. The results showed that the surface of the needle valve was covered with C deposits of varying thicknesses.

Figure 7
Table 5

3.4. Mechanism of carbonaceous deposition

The formation of carbonaceous deposit could be further understood by studying the soot particles extracted from the oil sump of the mode S195 diesel engine. **Figure 8** shows the HRTRM images of soot particles of diesel fuel and emulsified biomass fuel. It was found that the soot particles from both fuels were sphere-like in structure and were linked in a chain. The average diameter of the primary soot particles were about 38 nm, measured from the images using the Nano measurer software, which was similar to the results from the TEM images given in [32,33].

Figure 8
Figure 9

In general, the Raman spectrum is usually used to characterize the graphite degree of carbon materials. For the extracted carbon materials there were two strong overlapping peaks within 800-2000cm^{-1} as the wavelength of incident light λ_o = 532 nm. One peak was located at 1350cm^{-1}, another at 1580 cm^{-1} where Peak D (1350 cm^{-1}) corresponded to the carbon structure with a non-ordered state. Peak G (1580 cm^{-1}) corresponded to the graphite with an order structure. The ratio I_D/I_G gives an indication of the degree of graphite with a non-ordered state, which was calculated using a Gaussian curve fitting algorithm [15]. **Figure 9** shows the Raman analysis results of soot particles from diesel fuel and emulsified biomass fuel. It was found the I_D/I_G of emulsified biomass fuel was less, which means its graphite degree was higher. It was also consistent with that of XRD spectra.

The Raman analysis was consistent with the SEM/EDS, XRD and GC-MS results. The crystal state of carbonaceous deposition from the biomass fuel was higher than the diesel deposits, which caused the higher denser bio-oil deposit and was easier to aggregate. The more complex functional groups in the biomass fuel resulted in a greater tendency for polymerization and a higher adherence of the carbonaceous deposits from the biomass fuel. Thus, the way to solve the dense aggregation of carbonaceous deposits is to degrade the crystal state, and control adherence by variation of the functional groups.

4. Conclusions

(1) The carbonaceous deposition of from the emulsified biomass oil/diesel blended fuel was greater than that of diesel. The diameter of deposited carbon agglomerated particulates was approximately 10 μm to 30 μm with diesel and 50 μm with the emulsified biomass oil/diesel blend.

(2) Carbonaceous deposits from both fuels consisted of amorphous carbon. A crystalline order of carbon deposits was observed for the emulsified biomass oil/diesel blend, which formed thicker carbon deposits compared with diesel for similar engine conditions.

(3) The C and H elements within the carbonaceous deposit from the biomass oil/diesel blend were higher than that from diesel. The O content in the deposit from the biomass oil/diesel blend was lower than that from diesel. S, K, and Zn were found in the deposits and were derived from the

combustion of the additives of the lubricating oil.

(4) The mechanism of carbonaceous deposition could be attributed to the higher O content of more functional groups, thus leading to an ease in polymerization and condensation and the formation of high viscosity matter that was carbonized and deposited on the nozzle surfaces.

Acknowledgements

The authors wish to express their thanks to Mr. Xiangyang Wang, Ms. Tianxia Liu and Ms. Yinyang Shi for their assistance in the experimental analyses and with the discussion. The financial support of the National Natural Science Foundation of China (Grant Nos. 51275143 and 51405124), The Research Fund for International Young Scientists, NSFC (Grant No. 51450110436) and China Postdoctoral Science Foundation (Grant No. 2014M560505) are also gratefully acknowledged.

References

[1] Yuan Z, Wu C, Ma L. Biomass energy utilization principles and techniques. Beijing: Chemical Technology Press; 2005.

[2] Celik I, Sensogut C, Ceylan N. The effects of biodiesel usage on the components of an engine. Int J Global Energy Issues 2008; 29(3): 303-13.

[3] Wo HZ, Hu XG, Wang H, Xu YF. Cavitation erosion in injection nozzle of diesel engine. In: Davim JP, editor. Wear of advanced materials, London: ISTE/Wiley; 2011, p. 119-62.

[4] Xu YF, Hu XG, Li WD, Shi YY. Preparation and characterization of bio-oil from biomass. In: Shaukat S, editor. Progress in biomass and bioenergy production. Rijeka: InTech - Open Access Publisher; 2011, p. 197-22.

[5] Tan H, Wang S, Luo Z, Ceng K. Experimental research on biomass flash pyrolysis for bio-oil in a fluidized bed reactor. Agric Mach 2005; 36(4): 30-8.

[6] Park SH, Suh HK, Lee CS. Nozzle flow and atomization characteristics of ethanol blended biodiesel fuel. Renew Energy 2010; 35: 144-50.

[7] Hu E, Hu X, Wang X, Xu Y, Dearn K, Xu H. On the fundamental lubricity of 2,5-dimethylfuran as synthetic engine fuel. Tribol Int 2012; 55: 119-25.

[8] Zhu XF, Zheng JL, Guo QX, Zhu QS. Property, up-grading and utilization of bio-oil from biomass. Eng Sci 2005; 7(9):83-8.

[9] Xu Y, Yu H, Wei X, Cui Z, Hu X, Xue T, et al. Friction and wear behaviors of a cylinder liner-piston ring with emulsified bio-oil as fuel, Tribol Trans 2013; 56(3): 359-365.

[10] Sipila K, Kuoppala E, Fagemas L, Oasmaa A, Characterization of biomass-based flash pyrolysis oils. Biomass & Bioenergy 1998; 14(2): 103-13.

[11] Chiaramontia D, Boninia M, Fratinia E, Tondib G, Gartnerc K, Bridgwaterd AV, et al. Development of emulsions from biomass pyrolysis liquid and diesel and their use in engines-Part 2: tests in diesel engines. Biomass & Bioenergy 2003; 25: 101-11.

[12] Hu E, Hu X, Xu Y, Yu H, Zhu X. On the compatibility between biomass-fuel and elastomer. Corrosion 2012; 68(12): 1108-18.

[13] Hu XG, Xu YF, Wang QJ, Jiang ST, Zhu XF. Tribological performance of refined biomass-oil pyrolysis from rice straw. J Synth Lubri 2008; 25(3): 95-104.

[14] Patel M, Ricardo C L A, Scardi P, Aswath P B. Morphology, structure and chemistry of extracted diesel soot -Part I: Transmission electron microscopy, Raman spectroscopy, X-ray photoelectron spectroscopy and synchrotron X-ray diffraction study, Tribol Int 2012; 52 : 29–39.

[15] Uy D, Ford M A, Jayne D T, Neill A E O, Haack L P, Hangas J, Jagner M J, Sammut A, Gangopadhyay A K. Characterization of gasoline soot and comparison to diesel soot: Morphology, chemistry, and wear, Tribol Int 2014; 80: 198-209.

[16] La Rocca A, Di Liberto G, Shayler P J, Fay MW. The nanostructure of soot-in-oil particles and agglomerates from an automotive diesel engine, Tribol Int 2013; 61: 80-7.

[17] Barker J., Richards P., Snape C., Meredith W. Diesel injector deposits – An issue that has evolved with engine technology. SAE Paper No: 2011-01-1923.

[18] Barker, J., Snape, C., and Scurr, D., Information on the Aromatic Structure of Internal Diesel Injector Deposits From Time of Flight Secondary Ion Mass Spectrometry (ToF-SIMS), SAE Technical Paper 2014-01-1387.

[19] Barker J., Innospec J. R., Snape C., Scurr D., Meredith W. Spectroscopic studies of internal injector deposits (IDID) resulting from the use of non-commercial low molecular weight polyisobutylenesuccinimide (PIBSI). SAE Paper No: 2014-01-2720.

[20] Mendiratta RL, Singh D. Effect of base oil and additives on combustion chamber and intake valve deposits formation in IC engine. SAE Paper No: 2004-28-0089.

[21] Parsinejad F, Biggs W. Direct injection spark ignition engine deposit analysis: Combustion chamber

and intake valve deposits. SAE Paper No: 2011-01-2110.

[22] Zerda TW, Yuan X, Moore SM, Leon y Leon CA. Surface area, pore size distribution and microstructure of combustion engine deposits. Carbon 1999; 37(12): 1999-2009.

[23] Zerda TW, Yuan X, Moore SM. Effects of fuel additives on the microstructure of combustion engine deposits. Carbon 2001; 39(10): 1589-97.

[24] Kalghatgi GT. Combustion chamber deposits and knock in a spark ignition engine-some additive and fuel effects. SAE Paper No: 962009.

[25] Fay M W, La Rocca A, Shayler PJ, TEM and HRTEM of Soot-in-oil particles and agglomerates from internal combustion engines, Journal of Physics: Conference Series, 2014, 522: 012072 doi:10.1088/1742-6596/522/1/012072

[26] Sadezky A, Muckenhuber H, Grothe H, Niessner R, Poschl U. Raman microspectroscopy of soot and related carbonaceous materials: Spectral analysis and structural information. Carbon 2005; 43: 1731-42.

[27] Zhang D. Study on the application of emulsified on the engine and combustion mechanism. Diss Dalian Univ Tech 2002.

[28] Randy L. Vander Wal, Vicky M. Bryg and Michael D. Hays. Fingerprinting soot (Towards Source Identification) physical structure and chemical composition, J. Aerosol Sci., 20110, 41:108-17.

[29] Lapuerta M., Rodrıguez-Fernandez J., Agudelo J. R., Diesel particulate emissions from used cooking oil biodiesel, Bioresource Technol,2008, 99: 731–40

[30] La Rocca A., Di Liberto G., Shayler P., Parmenter C., Fay M. A novel diagnostics tool for measuring soot agglomerates size distribution in used automotive lubricant oils. SAE Int J Fuels Lubr, 2014, 7(1) : 2014-01-1479.

[31] Celik I, Aydin O, Effects of B100 biodiesel on injector and pump piston. Tribol Trans 2011; 54: 424-31.

[32] Hu E, Hu X, Liu T, Liu Y, Song R, Chen Y. Investigation of morphology, structure and composition of biomass-oil soot particles, Appl Surf Sci 2013; 270: 596-603,

[33] La Rocca A., Di Liberto G., Shayler P.J., Parmenter C.D.J., Fay M. W. Application of nanoparticle tracking analysis platform for the measurement of soot-in-oil agglomerates from automotive engines. Tribol Int, 2014, 70: 142–7.

Captions for Tables and Figures

Table 1 Physical and chemical properties of diesel and emulsified fuel

Table 2 Main technical specifications of Model S195 diesel engine

Table 3 Elements analysis of the carbon deposits

Table 4 EDS analysis results on the surface of needle valve seats with two fuels

The results are corresponds to the points cross-shaped in Figure 6 respectively

Table 5 EDS analysis results on the different surface regions of needle valve

Point cross-shaped in Figure 7 (a) was not covered with C deposits; Point cross-shaped in Figure 7 (b) was covered with C deposits

Figure 1 Optical images the of nozzles and needle valves showing and the surface thickness of carbon deposits after tests with two fuels

(a) $0^{\#}$ diesel (b) Emulsified fuel

Figure 2 Optical microscopy images of end face of nozzles after tests with two fuels

(a) 0# diesel (b) Emulsified fuel

Figure 3 XRD analysis results of carbon deposits

Figure 4 SEM images of the end face of the needle valve seat after utilization of the two fuels

(a) $0^{\#}$ diesel (b) Emulsified fuel

Figure 5 SEM images of needle valve sealing surface after the tests with the two fuels

(a) $0^{\#}$ diesel (b) Emulsified fuel

Figure 6 SEM images and EDS analysis regions of end face of the needle valve seat after utilization of the two fuels

(a) $0^{\#}$ diesel (b) Emulsified fuel

Figure 7 SEM images and EDS analysis regions of needle valve after utilization of emulsified fuel

(a) Region 1 (b) Region 2

Figure 8 HRTRM images of soot particles of diesel fuel and emulsified biomass fuel

(a) $0^{\#}$ diesel (b) Emulsified fuel

Figure 9 Raman results of soot particles from diesel fuel and emulsified fuel

EF: emulsified fuel; DF: diesel fuel

Table 1

Items	0# Diesel	Emulsified fuel	Test standards
Flash point (^{o}C)	55	50	ASTMD93
Kinematical viscosity (40^{o}C, mm^{2}/s)	2.92	3.09	ASTMD445
Acid number(mgKOH/g)	0.12	1.52	ASTMD664
Sulfur content (wt%)	0.25		ASTMD4294
Density (20^{o}C, kg/mm^{3})	817	743	ASTMD4052
Water content (V/V%)	Trace	Trace	ASTMD6304
Gross heat value (MJ/kg)	42.2	41.7	ASTM D240

Table 2

MODEL	S195
Type	Single cylinder, horizontal, 4-stroke
Cylinder diameter*piston stroke	95*115
Piston exhaust volume	0.815L
Rated output Power/rmp	9.7kw/2000r/min
Cooling method	Water
Starting method	Hand
Net weight (kg)	145
Size (mm)	866*412*639
Compression ratio	20:1
Lubrication system	Combined pressure and splash
Combustion system	Swirl
Output (HP/rpm)	12/2000
Piston total displacement (L)	0.815
Specific fuel consumption(g/kW.h)	≤287
Injection pressure (MPa)	12.6

Table 3

Items	C	H	N	O
Diesel	67.57567	5.175667	15.27833	11.970333
Emulsified fuel	74.05667	6.605333	14.87967	4.458327

Table 4

Diesel			Emulsified fuel		
Element	Weight (wt%)	Atomic (%)	Element	Weight (wt%)	Atomic (%)
C	23.93	33.48	C	25.87	37.86
O	55.05	57.81	O	48.64	53.43
S	3.71	1.94	S	3.24	1.78
Ca	2.73	1.14	Ca	0.94	0.41
Fe	7.32	2.20	Fe	8.55	2.69
Zn	2.71	0.70	Zn	10.51	2.83
Mg	1.53	1.06	K	2.25	1.01
Si	0.54	0.33			
P	2.48	1.35			
total	100.00		total	100.00	

Table 5

No C-Deposit			C-Deposit		
Element	Weight (wt.%)	Atomic %	Element	Weight (wt.%)	Atomic %
C	8.68	30.63	C	17.34	32.45
Cr	1.83	1.49	O	34.51	48.49
Fe	88.69	67.31	S	0.94	0.66
Co	0.80	0.58	Cl	0.36	0.23
			K	2.65	1.52
			Ca	2.28	1.28
			Cr	0.39	0.17
			Fe	15.69	6.32
			Zn	25.84	8.89
Totals	100.00		Totals	100.00	

(a)	(b)
Fig. 1	

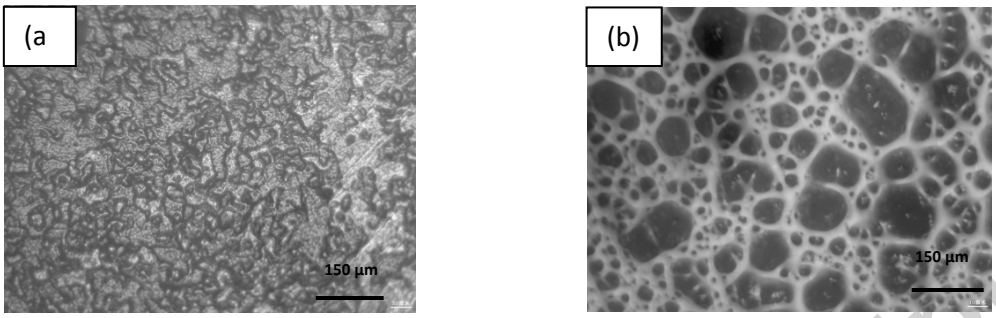

Fig. 2

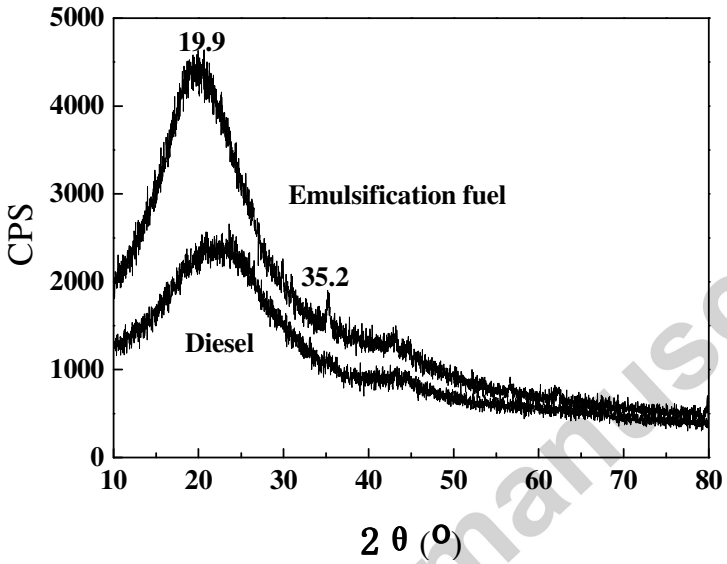

Fig. 3

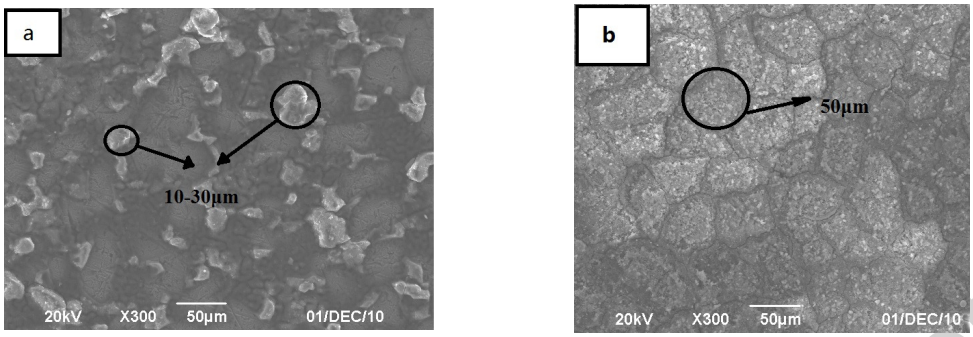

Fig. 4

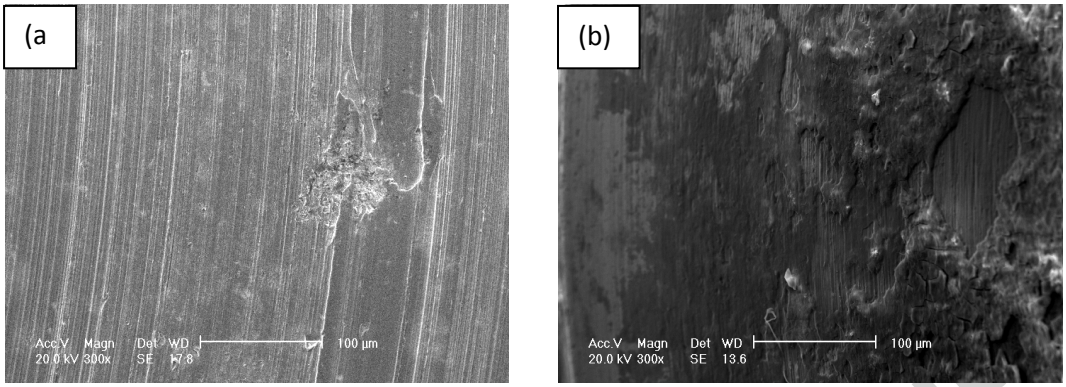

Fig. 5

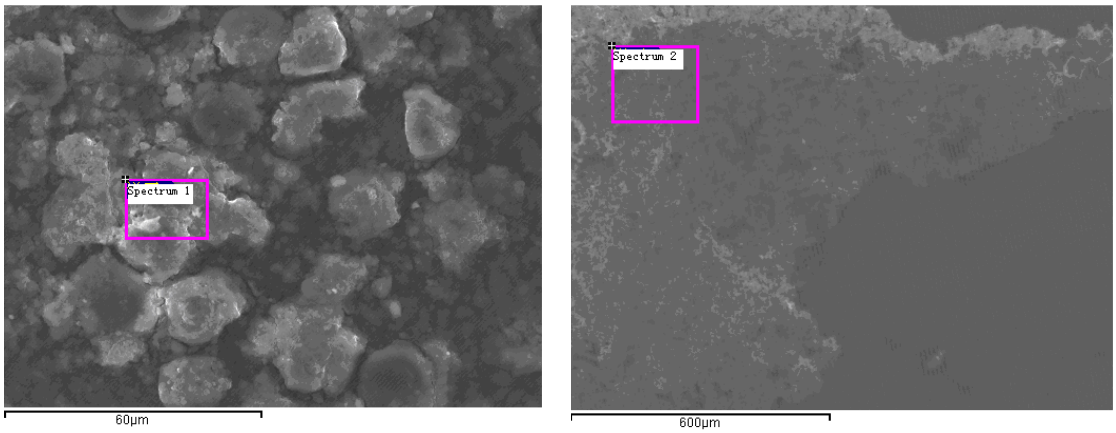

(a) (b)

Fig. 6

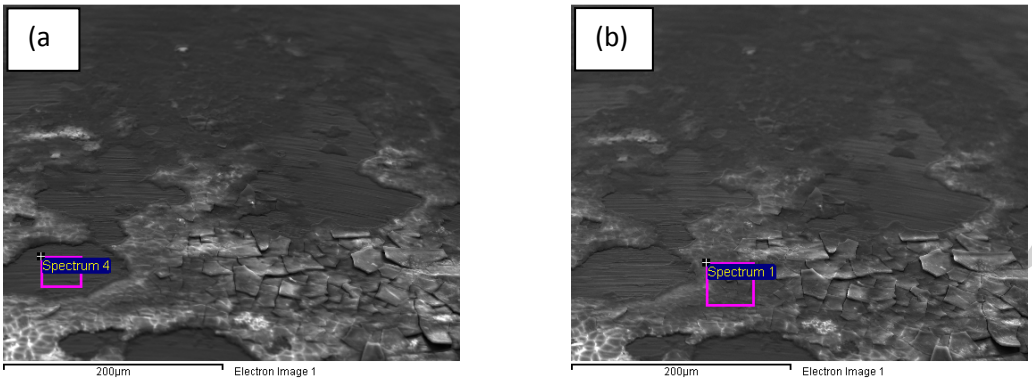

Fig. 7

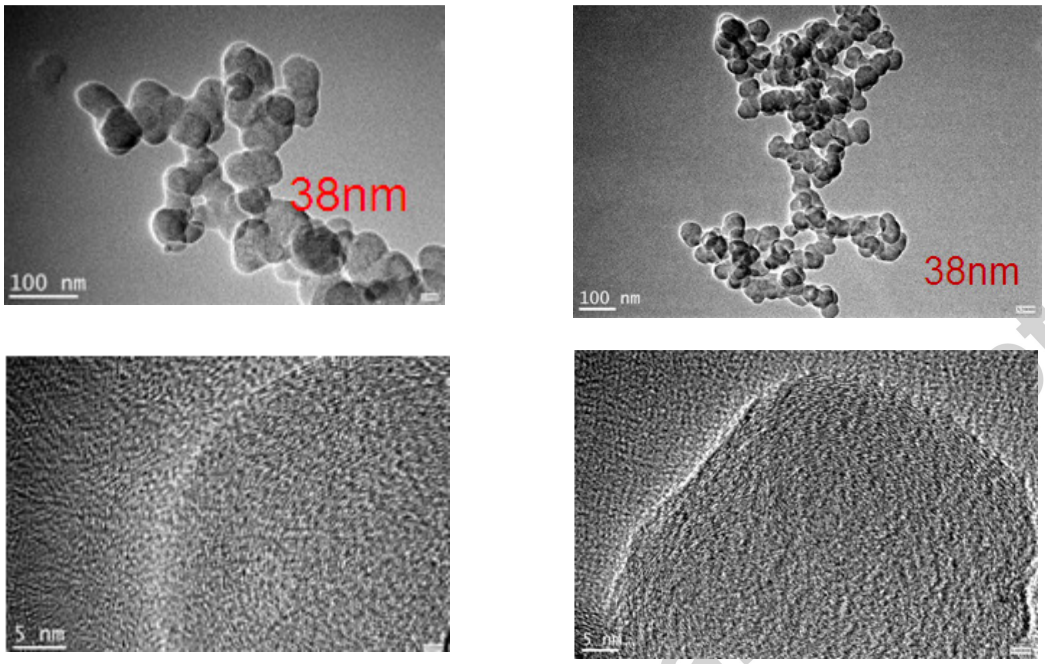

(a) (b)

Fig. 8

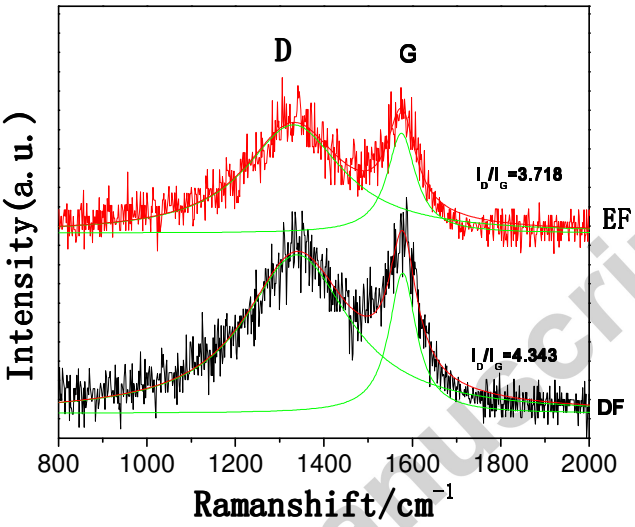

Fig. 9

Research Highlights

- The carbon deposit was mainly consisted of amorphous carbon.
- The diameter of carbon particulate was 50 μm with biomass-oil/diesel blend.
- Both C and H elements on the carbon deposit were higher, the oxygen was lower.
- The formation of carbon deposition was attributed to the higher oxygen content.